# A Novel Core Region, Lacking Heptose and Phosphate, of the Lipopolysaccharide from the Gram-Negative Bacterium *Pseudomonas cichorii* (*Pseudomonadaceae* RNA Group 1)

**Cristina De Castro,[a] Antonio Molinaro,*[a] Rosa Nunziata,[a] Rosa Lanzetta,[a] Michelangelo Parrilli,[a] and Otto Holst[b]**

**Keywords:** Core oligosaccharide / Lipopolysaccharide / Molecular modelling / NMR spectroscopy / Phytopathogenic bacteria / *Pseudomonas cichorii*

The extracted lipopolysaccharides (LPSs) fraction of the plant-pathogenic bacterium *Pseudomonas cichorii* contained two different molecules, the first of them an LPS possessing an O-specific polysaccharide made up of four 2-acetamido-2,6-dideoxy sugars linked linearly in a tetrasaccharide repeating unit. The structure of the second LPS component is reported here: it was of the rough form and contained a novel type of core region. The rough form LPS of *Ps. cichorii* was de-*O*-acylated by mild hydrazinolysis and then de-*N*-acylated with hot 4 M KOH. The oligosaccharide representing the complete carbohydrate backbone of the LPS was isolated by high-performance anion-exchange chromatography. Its structural characterization employed compositional and methylation analyses, matrix-assisted laser desorption/ionisation mass spectrometry and $^{1}H$, $^{13}C$ and $^{31}P$ NMR spectroscopy, with application of various 1D and 2D experiments. The carbohydrate backbone of this core region consisted of a hexasaccharide that contained no heptoses, being made up of L-Rha*p*, D-Glc*p*N and D-Gal*p*N, besides the characteristic α-(2→4)-linked 3-deoxy-D-*manno*-oct-2-ulosonic acid (Kdo) disaccharide. The first Kdo residue linking the core region to the lipid A was substituted by a Gal*p*N residue. This core region thus represents one of the rather few cases in which this position is not substituted by a *manno*-configured sugar. The structure of the LPS carbohydrate backbone is shown in Scheme 1. If not stated otherwise, sugars were D-configured pyranoses. Kdo is 3-deoxy-D-*manno*-oct-2-ulosonic acid. The lipid A backbone is *N*- and *O*-acylated in the LPSs. – Molecular modelling studies of the LPS carbohydrate backbone and of some of its parts were performed, yielding a preferred conformation that was surprisingly inflexible between the two Kdo residues.


## Introduction

Lipopolysaccharides (LPSs) are crucial amphiphilic constituents of the outer membrane of the Gram-negative bacterial cell wall.[1] Structurally, in their smooth forms (S-LPSs) they comprise three regions: the O-specific polysaccharide (or O-antigen), the oligosaccharide region (core-region) and the glycolipid part (lipid A). Rough-form (R) LPSs do not possess an O-specific polysaccharide and are named lipooligosaccharides (LOSs). LOSs, possessing mutations in the genes encoding the O-specific polysaccharide biosynthesis or transfer, may occur in both wild and laboratory strains.

α-L-Rha-(1→3)-β-GlcNAc-(1→3)-α-GalNAc-(1→5)-α-Kdo-(2→6)-β-GlcN4*P*-(1→6)-α-GlcN1*P*

4 ↑ 1 β-GlcNAc

4 ↑ 2 α-Kdo

Scheme 1

The core regions comprise oligosaccharides mostly composed of up to 15 monosaccharides[2–4] and may be divided into two regions: the inner core, made up of characteristic sugars such as 3-deoxy-D-*manno*-oct-2-ulosonic acid (Kdo) and L-*glycero*-D-*manno*-heptose (Hep), and the outer core, which contains more common sugars. Whereas Kdo, which always links the core region to lipid A, is always present, the heptose residues may be absent. In LOSs, the core oligo-

[a] Dipartimento di Chimica Organica e Biochimica, Università degli Studi di Napoli "Federico II",
Via Cinthia, 80126 Napoli, Italy
Fax: (internat.) +39-081-674393
E-mail: molinaro@unina.it
[b] Division of Structural Biochemistry, Research Center Borstel, Parkallee 22, 23845 Borstel, Germany
Supporting information for this article is available on the WWW under http://www.eurjoc.org or from the author.

saccharide is the external saccharide part of the molecule and so is involved in interaction with the external environment. In particular, it possesses antigenic properties and it is thought to modulate the toxic activities of the lipid A portion. In phytopathogenic bacteria, LPSs enhance the bacterial resistance to plant-derived antimicrobial compounds, which can give rise to particular plant defence-related responses. Plant response to subsequent bacterial inoculation can also be altered by preinoculation with LPSs.[5] In addition, the LPS structure may play a key role for the virulence of bacteria.

*Pseudomonas cichorii* causes a disease known as "varnish spot" in lettuce.[6] It was originally isolated from chicory[7] and subsequently reported to be present on many other hosts, such as cabbage, tomato, celery, tobacco, coffee and several ornamental plants, grown either in open fields or in greenhouses. On lettuce the disease is characterized by large, necrotic, brown-blackish areas that occur on the blades and petioles of leaves. *P. cichorii* produces both smooth- and rough-form LPSs. The O-specific polysaccharide of the smooth-form LPS was identified as a heteropolymer made up of a linear tetrasaccharide repeating unit.[8] In this paper, the structural characterization of the carbohydrate backbone of the rough-form LPS has been achieved by chemical analyses, Matrix-Assisted Laser Desorption/Ionisation-Time-of-Flight (MALDI-TOF) mass spectrometry, two-dimensional NMR spectroscopy and molecular modelling.

## Results

### Analyses of the Core Fraction Obtained from Acetic Acid Hydrolysis

In exploitation of the acid lability of Kdo, an aliquot of the LPS fraction was hydrolysed with aqueous 1% acetic acid and then centrifuged. The precipitate was identified as the lipid A made up of a 1,4′-bis(phosphorylated) GlcN disaccharide backbone substituted by C12:0(3-OH), C12:0(2-OH) and C12:0.[9] After gel-permeation chromatography of the supernatant, the core oligosaccharide fraction was obtained, and compositional analysis revealed the presence of Kdo, GalN, GlcN and Rha. No heptoses were detected. Methylation analysis yielded the derivatives of terminal Rha and GlcN, 3-substituted GlcN, 3,4-disubstituted GalN and 5-substituted Kdo (in small amounts). Colorimetric determination of the organic bound phosphate content and $^{31}P$ NMR analysis of the oligosaccharide fraction gave negative results, so the core region was free of phosphate. The $^{1}H$ NMR spectrum of the product obtained on acetic acid hydrolysis showed signals of *N*-acetyl groups present at $\delta = 1.9-2.0$ ppm, suggesting that the 2-amino functions were *N*-acetylated (data not shown). Furthermore, a MALDI-TOF mass spectrum (Figure 1a) of this product gave a major molecular ion at $m/z = 991.7$ [M − H]$^-$ and a minor one at $m/z = 973.9$ [[M − H]$^-$], consistent with the presence of a pentasaccharide chain made up of

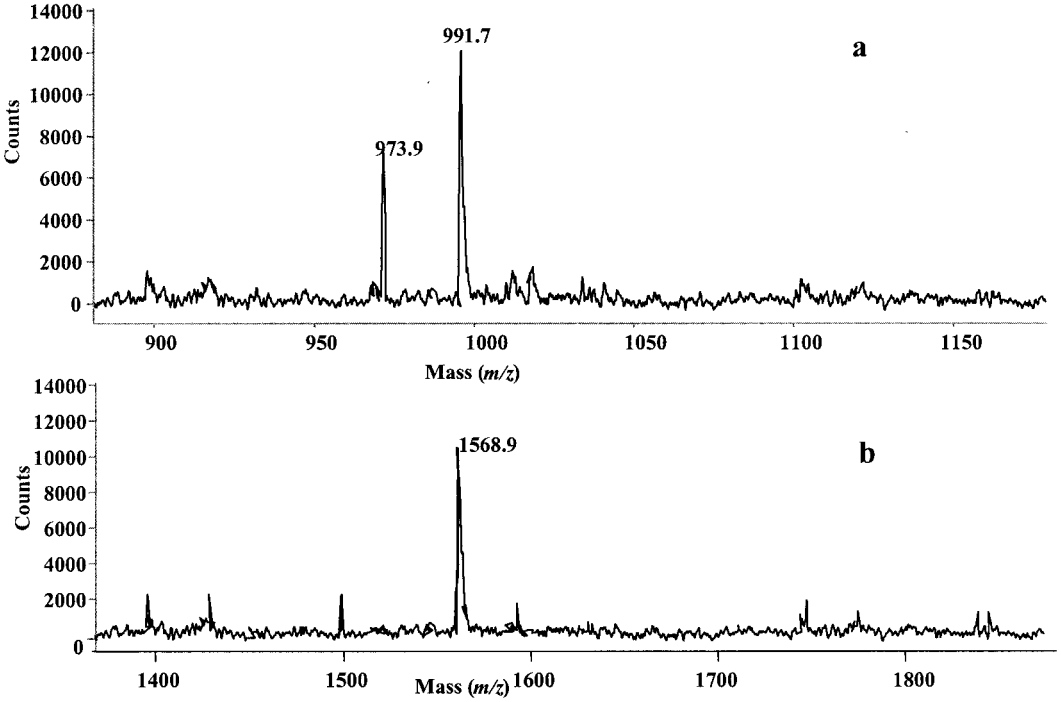


Figure 1. Negative-ion MALDI-TOF mass spectra of the product obtained from LPSs of *Ps. cichorii* by acetic acid hydrolysis (a), and of oligosaccharide **1** (b)

  

three *N*-acetyl hexosamine components, a Kdo residue and a deoxy monosaccharide (rhamnose). The second ion ($\Delta m/z = 18$) was most probably due to Kdo residue present as *anhydro* derivative.

### Isolation and Characterization of Oligosaccharide 1

Oligosaccharide **1**, consisting of core-lipid A bis(phosphorylated) oligosaccharide, was isolated by gel-permeation chromatography and high-performance anion-exchange chromatography (HPAEC) after complete deacylation of the LPS. Compositional analysis identified D-GalN, D-GlcN and L-Rha, and Kdo. Methylation analyses of the oligosaccharide yielded the derivatives of terminal Rha and terminal GlcN, 3-substituted GlcN, 6-substituted GlcN, 3,4-disubstituted GalN, and 4,5-disubstituted and terminal Kdo. Additionally, traces of an 8-substituted Kdo and of terminal Glc were found.

### NMR Spectroscopy of Oligosaccharide 1

The structure of oligosaccharide **1** was established by $^{1}H$, $^{31}P$ and $^{13}C$ NMR spectroscopy. Chemical shifts were assigned by utilisation of DQF-COSY, TOCSY, NOESY, ROESY, HMQC, HMBC and HMQC-TOCSY experiments. Anomeric configurations were assigned on the basis of the observed chemical shifts and of $^{3}J_{H1,H2}$ values determined from the DQF-COSY experiment. The data are presented in Table I.

All sugars were identified as pyranoses, on the basis of their $^{1}H$ and $^{13}C$ NMR chemical shifts and of an HMBC spectrum, which showed intra-residual scalar connectivities between H-1/C-1 and C-5/H-5 of residues A−F.

The anomeric region of the $^{1}H$ NMR spectrum (Figure 2) contained 6 anomeric signals (A−F), representing one 6-deoxy hexose and five hexosamine residues.

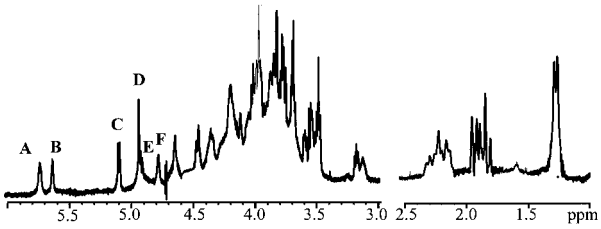


Figure 2. 1D $^{1}H$ NMR spectrum of oligosaccharide **1**; the spectrum was recorded in $D_2O$ at 600 MHz and 30 °C

Their identification was possible through the complete assignment of all proton signals and the determination of the $^{3}J_{H,H}$ vicinal coupling constant values. Three hexosamine residues (residues C, E and F) possessed the β-*gluco* configuration. This assumption was also supported by a NOESY experiment that showed intra-residual NOE connectivities from H-1 to H-3 and to H-5 for these sugar residues. One hexosamine residue (A) possessed the α-*gluco* configuration, the last hexosamine (B) the α-*galacto* configuration. The 6-deoxy hexose (D) was α-*manno*-configured, and so was rhamnose. The characteristic H-3 signals of two Kdo residues were present at 1.853 ppm ($H\text{-}3_{ax}$) and 2.226 ppm ($H\text{-}3_{eq}$) (residue H) and 1.905 ppm ($H\text{-}3_{ax}$) and 2.220 ppm ($H\text{-}3_{eq}$) (residue G). Their α configurations were established on the basis of the chemical shifts of their $3_{eq}$ and H-5 protons and by the values of the $^{3}J_{H7,H8a}$ and

Table 1. $^{1}H$, $^{13}C$ NMR (bold) chemical shifts and anomeric coupling constants (italic) of sugar residues of the core-lipid A backbone (oligosaccharide **1**) of LPS from *Ps. cichorii*; chemical shifts (ppm) are expressed relative to acetone ($^{1}H$, 2.225 ppm, $^{13}C$, 31.45 ppm, at 30 °C): monosaccharides are labelled as shown in Figure 5

| Residue | H-1/C-1 | H-2/C-2 | H-3/C-3 | H-4/C-4 | H-5/C-5 | H-6/C-6 | H-7/C-7 | H-8/C-8 |
|---|---|---|---|---|---|---|---|---|
| GlcN | 5.732 | 3.471 | 3.950 | 3.640 | 4.105 | 4.253/3.856 | | |
| **A** | *3.3* Hz | | | | | | | |
| | **91.9** | **55.2** | **70.6** | **70.9** | **69.9** | **71.5** | | |
| GalN | 5.630 | 3.911 | 4.468 | 4.664 | 4.199 | 3.850/3.960 | | |
| **B** | *3.3* Hz | | | | | | | |
| | **98.2** | **51.7** | **78.6** | **76.9** | **67.9** | **61.5** | | |
| GlcN | 5.100 | 3.117 | 3.736 | 3.565 | 3.518 | 3.980/3.640 | | |
| **C** | *8.1* Hz | | | | | | | |
| | **101.8** | **57.2** | **73.6** | **70.6** | **76.1** | **62.3** | | |
| Rha | 4.923 | 3.826 | 3.758 | 3.487 | 4.010 | 1.280 | | |
| **D** | **100.9** | **71.5** | **73.3** | **72.9** | **70.1** | **17.6** | | |
| GlcN | 4.908 | 4.010 | 3.700 | 3.825 | 3.596 | 3.686/3.932 | | |
| **E** | *7.7* Hz | | | | | | | |
| | **102.8** | **56.2** | **82.6** | **71.8** | **76.1** | **62.3** | | |
| GlcN | 4.771 | 3.175 | 3.390 | 3.750 | 3.500 | 3.527/3.625 | | |
| **F** | *8.0* Hz | | | | | | | |
| | **102.0** | **56.7** | **75.0** | **73.8** | **76.0** | **64.3** | | |
| Kdo | | | 1.905/2.220 | 4.144 | 4.090 | 3.654 | 4.000 | 3.750/3.913 |
| **G** | **175.2** | **101.0** | **34.9** | **66.8** | **67.0** | **73.0** | **71.0** | **64.4** |
| Kdo | | | 1.853/2.226 | 4.298 | 4.200 | 3.754 | 3.856 | 3.663/3.892 |
| **H** | **176.5** | **100.5** | **34.3** | **70.3** | **72.7** | **72.9** | **70.7** | **64.1** |

  

$^3J_{H7,H8b}$ coupling constants, of 7.1 and 3 Hz, respectively.[10,11]

The $^{13}C$ NMR chemical shifts were assignable through an HMQC experiment, using the assigned proton resonances. Six anomeric signals were identified (Table 1) together with a large number of carbon signals relative to ring carbon, two methylene carbon signals belonging to Kdo units and the methyl signal of a rhamnose residue. Low-field shifted signals indicated substitutions at O-6 of residues A and F, at O-5 and O-4 (H), at O-3 and O-4 (B), and at O-3 (E), while C, D and G were terminal sugars. The sequence of the monosaccharide residues was determined from NOE data (Figure 3).

Dipolar couplings were found between H-1 of GlcN F and H-6 of GlcN A, H-1 B and H-5 H, and H-$8_{a,b}$ H, H-1 C and H-4 B, H-1 E and H-3 B and, finally, between H-1 D and H-3 E. In the case of Kdo units, which lack anomeric protons, the sequence was inferred from NOE contacts between the protons H-$3_{ax}$ and H-$3_{eq}$ of Kdo H and H-6 of Kdo G, characteristic of the sequence α-D-Kdo-(2→4)-α-D-Kdo.[12] As for the location of Kdo H, its linkage to unit F was deduced by taking into account the downfield shift of C-6−F (δ = 64.3 ppm, Table 1) indicating its substitution, which, by elimination, must be with residue H. Since the anomeric protons of glycosyl residues give dipolar couplings mostly, although not exclusively, with the proton at the linkage of the glycosylated position of the adjacent residue, the NOE data, together with the $^{13}C$ glycosylation shifts, confirmed the above linkages for each residue.

A *g*HMBC spectrum confirmed the assigned structure for oligosaccharide **1**, since it contained the required long-range correlations significant for the sequence of the residues and for the attachment points, in full accordance with methylation analysis and NOESY data. Together with intra-residual long-range connectivities, the inter-residual ones were between H-1/C-1 of F and C-6/H-6 of A, H-1/C-1 of B and C-5/H-5 of H, H-1/C-1 of C and C-4/H-4 of B, H-1/C-1 of E and C-3/H-3 of B, and H-1/C-1 of D and C-3/H-3 of E.

Two signals at δ = 2.5 ppm and 3.2 ppm were found in the $^{31}P$ NMR spectrum, and were assigned by means of a $^1H$-$^{31}P$ HMQC experiment to phosphate groups linked to O-4 of residue F and to O-1 of residue A, respectively. These assignments were in good agreement with the expected chemical shift of the respective proton and carbon signals geminal to a phosphate group.

A negative ion MALDI-TOF mass spectrum (see b in Figure 1) of oligosaccharide **1** gave a molecular ion at *m*/*z* = 1568.9 $[M - H]^-$, which indicated a molecule consisting of five hexosamine, two Kdo, two phosphate and one deoxyhexose residues.

## Conformational Analysis of Oligosaccharide 1

All NOE connectivities observed were confirmed by conformational analysis of the assigned structure. Oligosaccharide **1** (without GlcN disaccharide) was built with the aid of the MacroModel package and submitted to extensive MM3* force-field calculations.

All the disaccharide entities listed in Table 2 were constructed and subjected to a systematic search over all the possible Φ and Ψ combinations, performed by use of the DRIV utility in the MacroModel package (relaxed maps are available as Supporting Information, Figure S2−S10; for Supporting Information see also the footnote on the first page of this paper). The approach to Kdo mono- and oligosaccharide is discussed here comprehensively, due to the interesting results obtained. By the most commonly used approach, the Kdo carboxyl group was considered protonated, although under the NMR experimental conditions it is not. Actually, similar behaviour of glycoside bonds of acidic sugars in the neutral or ionic state has been found.[13] In the first part of this approach, the optimal dihedral angles around each glycosidic junction were evalu-

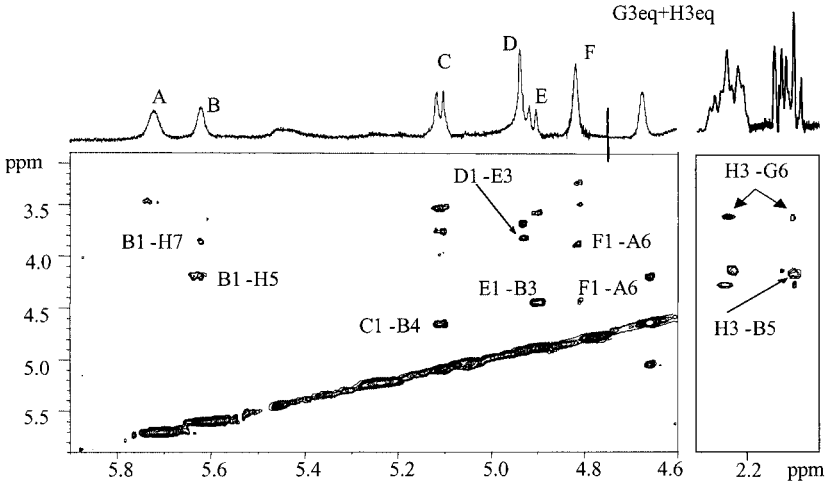


Figure 3. The anomeric and Kdo methylene regions of the 2D NOESY spectrum of oligosaccharide **1**; the spectrum was recorded in $D_2O$ at 600 MHz and 30 °C with a mixing time of 200 ms; the relevant inter-residual correlations are illustrated; the letters refer to the carbohydrate residues as shown in Figure 5 and Table 1, and the arabic numerals to the protons of the respective residues

  

Table 2. Optimal dihedral angles and corresponding energies of each glycosidic junction of the core oligosaccharide; the parameters were estimated with the DRIV option of the MacroModel package

| Glycosidic unit | Energy (kJ/mol) | Φ | Ψ |
|---|---|---|---|
| α-L-Rha-(1→3)-β-D-GlcN | 127.1 | +55.2 | +17.2 |
| | 130.1 | +36.4 | −51.6 |
| | 136.2 | −39.1 | −35.3 |
| β-D-GlcN-(1→3)-α-D-GalN | 84.8 | +59.0 | −28.6 |
| | 85.5 | +56.6 | +27.1 |
| | 94.1 | +163.1 | +7.5 |
| β-D-GlcN-(1→4)-α-D-GalN | 84.6 | +56.1 | +19.1 |
| α-D-GalN-(1→5)-α-D-Kdo[a] | 120.7 | −21.9 | +43.9 |
| | 124.6 | −49.4 | −6.7 |
| α-D-GalN-(1→5)-α-D-Kdo[b] | 123.3 | −21.9 | +43.9 |
| | 127.4 | −49.9 | −6.7 |
| α-D-Kdo-(2→4)-α-D-Kdo[a] | 148.6 | −54.3 | −17.2 |
| | 150.7 | −51.6 | +54.6 |
| | 153.7 | +54.3 | 0.0 |
| α-D-Kdo-(2→4)-α-D-Kdo[b] | 153.8 | −55.4 | −20.0 |
| | 159.1 | −62.0 | +31.8 |
| | 162.3 | +51.2 | +35.7 |
| α-D-GalN-(1→5)-[α-D-Kdo-(2→4)-]-α-D-Kdo[a,c] | 190.7 | −57.1 | −19.8 |
| | 196.9 | −52.5 | +34.5 |
| | 197.4 | +55.2 | +17.2 |
| α-D-GalN-(1→5)-[α-D-Kdo-(2→4)-]-α-D-Kdo[b,c] | 187.6 | −55.2 | +30.2 |

[a] Carboxyl orientation ($O_{carb.}C_1C_2O_2$) set to +60°. [b] Carboxyl orientation ($O_{carb.}C_1C_2O_2$) set to −60°. [c] DRIV performed over the Kdo-Kdo glycosidic junction.

ated. To start the conformational search, each monosaccharide was minimised and great care was dedicated to the Kdo residue, since the energies of this monosaccharide and the resulting disaccharide relaxed maps are influenced by the orientation of its carboxylic function. In particular, with setting of the dihedral angle $O_{carb.}C_1C_2O_2$ at +60°, the Kdo monosaccharide reached its global minimum ($E$ = 72.1 kJ/mol, Figure S1, S series refers to the Supporting Information available for this article; see also the footnote on the first page of this article) and the adiabatic map of the disaccharide α-D-Kdo-(1→4)-α-D-Kdo showed three different and intense minima (Figure S2). When the dihedral angle $O_{carb.}C_1C_2O_2$ was set to −60°, the monosaccharide energy reached the value of 74.6 kJ/mol and the resulting adiabatic map showed two intense minima and only a weak third one (Figure S3). The global minima of these two maps differed by about 2 kJ/mol, but shared similar dihedral angle values. The orientation of the carboxylic function of Kdo also influenced the energy value found for the disaccharide α-D-GalN-(1→5)-α-D-Kdo (i.e., when it was set to +60°, the global minimum of the corresponding disaccharide was 120.5 kJ/mol (Figure S4), otherwise (set to −60°) it was 123.3 kJ/mol (Figure S5). The two relaxed maps differed in the energies associated with each level, but the contours were roughly comparable.

An interesting result was observed on study of the inner core region: the trisaccharide unit α-D-GalN-(1→5)-[α-D-Kdo-(2→4)-]-α-D-Kdo. In this case, the GalN residue was accommodated according to its preferred conformation and two relaxed maps were calculated for the Kdo−Kdo glycosidic junction. In the first case the carboxyl orientation was set to +60° (Figure S6), in the second to −60° (Figure S7).

The first adiabatic map (Figure S6) showed three different minima, the lowest energy being 190.7 kJ/mol, characterized by the angles Φ = −57.1° and Ψ = −19.8°. This map was very similar to that of the disaccharide α-D-Kdo-(2→4)-α-D-Kdo possessing the same carboxyl orientation (Figure S2).

The second adiabatic map (Figure S7), in contrast with the results obtained for the corresponding disaccharide, showed one minimum with an energy of 187.6 kJ/mol and the dihedral angles Φ= −55.9° and Ψ = +30.2° previously found for the higher-energy conformation.

This result was quite unexpected, since the disaccharide with a Kdo residue possessing the less favourable carboxyl orientation had a global energy higher than that of the species with the favourable carboxyl orientation. However, this behaviour was reversed when the reducing Kdo was further substituted with an α-D-GalN residue in position 5, as present in the inner core region trisaccharide.

These results suggested that glycosidation of the disaccharide α-D-Kdo-(2→4)-α-D-Kdo with a GalN moiety introduces significant rigidity into the whole structure (one minimum versus the previous three) and also that there was a new preferred conformation different from that found for the simple disaccharide.

In order to obtain a complete picture of the flexibility of the molecule, two different conformers of oligosaccharide **1** (without phosphates on the lipid A moiety) were constructed with employment of the optimal dihedral angles reported in Table 2, differing only in the inner core region: in one case the carboxyl orientation was set to the optimal value found for the monosaccharide (+60°) and in the second case this function was drawn with the other orien-

  

tation (−60°), the glycosidic angles of the Kdo−Kdo subunit being selected accordingly in both cases. For simplicity of discussion, the two conformers are referred to as core+60 and core−60 and their starting energies (MM3 force-field, in vacuo, ε = 80) were 384.3 and 381.6 kJ/mol, respectively.

The two oligosaccharides were separately subjected to Molecular Dynamics simulation at 303 K for 8 ns, again with the MM3* force-field, and with water solvent approximation by use of the GB/SA model. This approach allowed analysis of long-range interactions between all the sugar residues, as well as possible transitions between different conformations. All the graphics extracted from the simulations are reported in the Supporting Information.

The outer core residues E, D and C behaved similarly in the simulations of the two conformers. The scattering of the Φ and Ψ values was very similar, as was the variation of the glycosidic *inter* proton distances (Figures S11−S13).

The inner core region behaviour was different and depended on the starting conformation used.

Analysis of core+60 indicated a rigidity around the glycosidic junction of the α-D-GalN-(1→5)-α-D-Kdo unit (B−C, Figure S14−S15), whereas the Φ, Ψ values of the α-D-Kdo-(2→4)-α-D-Kdo scattered around two different regions of the map (G−H, Figure S16). It is noteworthy that the carboxyl group of residue G preferred the +60° orientation, whereas that of H fell into the −60° state after 2 ns (Figures S16d and S16e, respectively) and did not revert to the original state.

In contrast with the above conformer form, core−60 showed some flexibility around the glycosidic junction α-D-GalN-(1→5)-α-D-Kdo (B−C, Figure S14a), whereas the Φ, Ψ values of α-D-Kdo-(2→4)-α-D-Kdo fell in only one region of the graphic (Figure S16a), similarly to what had been found for the adiabatic map of the trisaccharide (Figure S7). Moreover, the carboxyl orientation for both G and H was constant at −60° over all the simulation time.

In order to select the more representative dynamic data, ensemble average inter-proton distances for the whole molecule were extracted from both dynamic simulations and translated into NOE contacts by a full-matrix relaxation approach, and the predicted NOEs were then compared with those collected experimentally. Surprisingly, only the core−60 simulation showed excellent agreement with the experimentally observed data (Table 3). Core+60 was discarded as a representative structure because of the absence of NOE interactions between H4−$G3_{eq}$ (Figure S17d) and H5−G4 (Figure S17e) in the NOESY spectra.

From the above results, it appeared that the conformation adopted by this oligosaccharide can be depicted well by the conformer core−60. In particular, this structure possesses a marked inflexibility around the glycosidic linkage between the two Kdo residues (Figure 4).

This feature was quite surprising, since oligosaccharides usually exhibit rather high flexibility around their glycosidic linkages, especially when the residue is in a terminal position, as with Kdo **G** in this case. This behaviour is important for analysis of a probable recognition between this region of the molecule and a receptor. Usually, a receptor molecule possesses affinity only to one family of possible conformations of the molecule. The presence of different conformation families of the epitope hinders the binding process whereas the presence of only the preferential one improves the whole recognition process.

Table 3. Comparison of the predicted distances (Å) obtained by molecular dynamics simulations for core+60 and core−60 with distances measured in NOESY spectrum

| Protons | Core+60 | Core−60 | Experimental distances |
|---|---|---|---|
| D1E3 | 2.51 | 2.57 | 2.63 |
| E1B3 | 2.38 | 2.40 | 2.47 |
| C1E2 | 2.71 | 2.70 | 2.64 |
| C1B4 | 2.66 | 2.66 | 2.35 |
| B1H5 | 2.30 | 2.28 | 2.40 |
| B1H7 | 4.54 | 2.90 | 3.20 |
| $B5H3_{ax}$ | 2.39 | 2.36 | 2.70 |
| $G6H3_{ax}$ | 3.54 | 3.07 | 2.86 |
| $G6H3_{eq}$ | 2.60 | 2.21 | 2.45 |
| $H4G3_{eq}$ | 2.32 | 4.33 | − |
| H5G4 | 2.79 | 5.21 | − |

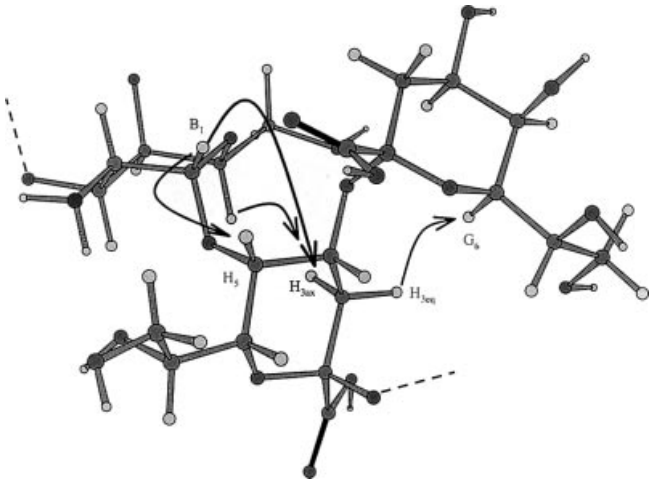


Figure 4. Stick and ball representation of a minimum-energy conformation of oligosaccharide **1**; for clarity, only the inner core moiety is depicted, the arrows indicate the main and more diagnostic NOE contacts found in the NOESY spectrum

In summary, the data have established the structure of oligosaccharide **1** (Figure 5) representing the carbohydrate backbone of the rough form LPS from *Ps. cichorii*.

## Discussion

According to 16S-RNA analyses, the *Pseudomonadaceae* family comprises five groups,[14] the first of which consists of authentic *Pseudomonas* bacteria, while the second contains the genus *Burkholderia. Pseudomonas cichorii* is a member of RNA group 1. In the core regions of all LPSs from authentic *Pseudomonas* elucidated to date (i.e., of LPSs from *Ps. aeruginosa* and *Ps. fluorescens*[2,3]), Hep residues are always present and the core regions are phos-

  

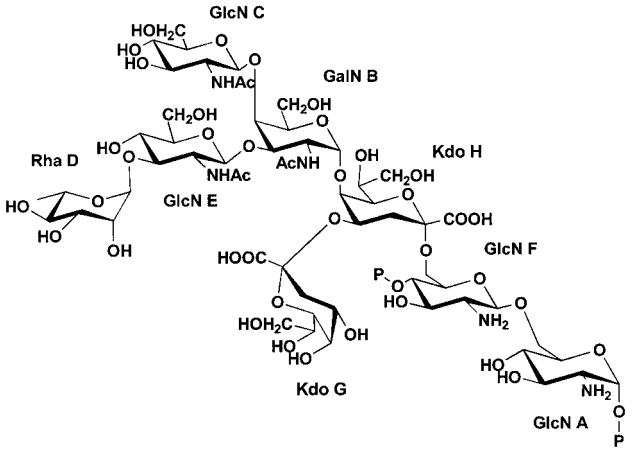


Figure 5. The structure of oligosaccharide **1** of the LPS from *Ps. cichorii*

phorylated, including the highest number of phosphate residues so far found in LPSs.[15] The first heptose residue is linked to C-5 of Kdo I and is generally substituted at O-3 by a second Hep, which carries a carbamoyl residue at O-7. Thus, all core regions of LPSs from *Pseudomonas* bacteria so far elucidated possess two Hep residues. The second Hep residue in all cases carries a GalN at O-3, its amino function frequently substituted by D-alanine. Depending on the LPSs, the GalN residue may carry various substituents, at position O-3 alone or at O-3 and O-4.

The structure of the core region of LPSs of a rough strain *Ps. cichorii* differed significantly from the core structures described above. Heptose and phosphate residues were definitely absent. A GalNAc residue disubstituted at O-3 and O-4 was still present, but this was directly linked to O-5 of Kdo. This is the first case in which O-5 of Kdo I is substituted by a residue bearing a *galacto* configuration. It was therefore important to study the three-dimensional structure of the molecule, which resulted in the above interesting conclusions.

Another element of originality in this core oligosaccharide structure relates to its low negative charge. Usually, the core regions of LPSs from various bacteria have been found to be negatively charged. In most cases, such charges are provided by phosphate groups and Kdo residues. In phosphate-free core regions, uronic acids are introduced. It is generally accepted that bivalent (metal or organic) ions act as counterparts to these negative charges and assemble ionic bridges between LPS molecules, which contribute to the rigidity and stability of the Gram-negative cell wall.[16] Since the core region of LPS from *Ps. cichorii* possessed only two weak negative charges provided by two Kdo residues, the contribution of the LPSs to cell wall stability should be of limited value. The bacterium should therefore possess other molecules and/or mechanisms to guarantee a stable and protective cell wall.

In summary, the structure of the core region of LPSs from the phytopathogenic *Ps. cichorii* differs notably from the core structures described earlier, and these structural peculiarities are reflected in the unique secondary structure of the oligosaccharide. Our data have shown that this molecule displays considerable rigidity in its inner region, which could be due to challenges of the external environment that the bacterium has to face.

## Experimental Section

**Bacteria and Bacterial LPS:** *Pseudomonas cichorii* strain 5707 (isolated from *Cichorium endiva* L.) was cultivated as described.[8] The dried cells (1.9 g) were extracted with hot phenol/water,[17] both phases of which were separately dialysed against distilled water and then lyophilised (yields: water phase, 84.6 mg; phenol phase, 77 mg; each about 4% of the bacterial dry mass). Both fractions were analysed by discontinuous SDS-PAGE electrophoresis (separating gel: 12%) with use of a miniprotean gel system (Bio-Rad). Samples (4 μg) were run at constant voltage (150 V) and were stained with silver nitrate according to Kittelberger.[18] The LPSs fraction was detected in the phenol phase and was further purified by gel-permeation chromatography with a column (1.5 × 90 cm) of Sephacryl HR 400 (Pharmacia), eluted at 0.4 mL·min$^{-1}$ with 50 mM $NH_4HCO_3$. The collected fractions were screened for their LPS content by SDS-PAGE. Positive fractions were combined to yield a LPS fraction (50 mg, 3% of the bacterial dry mass).

**Isolation of Oligosaccharides:** An aliquot of the LPSs (10 mg) was hydrolysed in 1% acetic acid (100 °C, 2 h) and the precipitate (lipid A) was removed by centrifugation (8000 × *g*, 30 min). The supernatant was separated by gel-permeation chromatography on a column (50 × 3 cm) of Sephadex G-50 (Pharmacia). Two fractions were obtained, the first of which eluted in the void volume and contained the O-specific polysaccharide (7.1 mg, 71% of the LPSs). A second fraction consisted of core oligosaccharides (2.5 mg, 25% of the LPSs).

For deacylation,[19] the LPSs (40 mg) were dissolved in anhydrous hydrazine (1.5 mL), stirred at 37 °C for 30 min, cooled, poured into ice-cold acetone (10 mL), and allowed to precipitate. The precipitate was then centrifuged (3000 × *g*, 30 min), washed twice with ice-cold acetone, dried, and then dissolved in water and lyophilised (32 mg, 80% of LPS). The sample was subsequently treated with 4 M KOH at 120 °C for 18 h. After desalting with the aid of a column (50 × 1.5 cm) of Sephadex G-10 (Pharmacia), the resulting poly-/oligosaccharide fraction (20 mg, 50% of the LPS) was further separated by gel-permeation chromatography with a column (50 × 3 cm) of TSK-40 (Merck) in pyridine/acetic acid/water (8:20:1000, by vol.). Two fractions were obtained, the first of which eluted in the void volume and contained the O-specific chain (13.1 mg, 33% of the LPS). The second fraction (4.1 mg, 10% of the LPS), which consisted of oligosaccharide material, was supplementarily purified by high-performance anion-exchange chromatography (HPAEC) on a column (4 × 250 mm) of CarboPac PA100 (Dionex) eluted at 1 mL·min$^{-1}$ with a linear gradient of 1−5% 1 M sodium acetate in 0.1 M NaOH over 120 min. Oligosaccharide **1**, representing the complete carbohydrate backbone of the lipid A-core region (1 mg, < 1% of the LPS), was obtained.

**General and Analytical Methods:** The determination of neutral sugars and their absolute configurations, as well as the determination of organic bound phosphate and of Kdo, were performed as reported.[20−23] For methylation analysis of the Kdo region,[24] oligosaccharide **1** was first *N*-acetylated with acetic anhydride (15 μL) in NaOH (0.5 M, 150 μL) for 10 min, then carboxy-methylated with methanolic HCl (0.1 M, 5 min) and consecutively with diazomethane in order to improve its solubility in DMSO. After methylation,

  

product **1** was hydrolysed with trifluoroacetic acid (2 M, 100 °C, 1 h), carbonyl-reduced with $NaB^2H_4$, carboxy-methylated as before, carboxyl-reduced with $NaB^2H_4$ (4 °C, 18 h), acetylated and analysed by GLC-MS.

Methylation of the complete core region was carried out as described above, and the sample was hydrolysed with trifluoroacetic acid (4 M, 100 °C, 4 h), carbonyl-reduced with $NaB^2H_4$, carboxy-methylated, carboxyl-reduced, acetylated and analysed by GLC-MS. A third methylation analysis was carried out on the core oligosaccharide fraction obtained from AcOH treatment as described above.

**Mass Spectrometry:** MALDI-TOF spectra were recorded as follows: 1 μL analyte solution in chloroform/trifluoroethanol (4:1) was mixed with 1 μL of matrix solution consisting of trihydroxyacetophenone in 0.2% trifluoroacetic acid, applied to the sample plate and dried. Mass calibration was performed by use of the molecular ions from bovine insulin at 5734.5 Da and a peptide at 1209.3 Da as external standards. Raw data were analysed by use of computer software provided by the manufacturer and are reported as average masses.

**NMR Spectroscopy:** For structural assignments of oligosaccharide **1**, 1D and 2D $^1H$ NMR spectra were recorded on a solution of 1 mg in 0.5 mL $D_2O$ with a Bruker DRX 600 spectrometer (operating frequency 600 MHz). Measurements were achieved at 30 °C, pD 10, relative to internal acetone [$\delta^1_H = 2.225$, $\delta^{13}_C = 31.07$ ppm]. $^{31}P$ NMR spectra were recorded with a Bruker DRX 400 spectrometer (operating frequency 162 MHz), fitted with a reverse probe, in the FT mode at 30 °C. Phosphoric acid (85%) was used as external standard ($\delta = 0.00$ ppm). Coupling constants were determined on a first order basis by 2D phase-sensitive double quantum-filtered correlation spectroscopy (DQF-COSY), measured by use of standard Bruker software.[25,26] Total correlation (TOCSY) and nuclear-Overhauser-enhancement (NOESY) spectroscopy were carried out in the phase-sensitive mode by the method of States et al.[27] The TOCSY experiment was carried out with a mixing time of 80 ms. The NOESY experiments were recorded with mixing times of 100, 200 and 300 ms, and the intensities were classified as strong, medium and weak, with use of cross-peaks from intra-ring proton-proton contacts for calibration. The $^1H$-$^{13}C$ correlations were measured in the inverse mode, by heteronuclear multiple quantum coherence (HMQC) and gradient selected heteronuclear multiple bond correlation (*g*HMBC) experiments with the aid of standard Bruker software.[28,29] The experiments were carried out in the phase-sensitive mode by use of States-time-proportional incrementation. A 60 ms delay was used for the evolution of long-range connectivities in the HMBC experiment. The $^1H$,$^{31}P$ correlations were measured in the inverse mode as HMQC.

**Molecular Mechanics and Dynamics Calculations:** Molecular Mechanics and Dynamics calculations were performed by use of the MM3* force-field as implemented in MacroModel 7.2, installed under the Red Hat 7.2 operative system. The MM3* force-field used[30] differs from the regular MM3 force-field in the treatment of the electrostatic term, since it uses charge-charge instead of dipole−dipole interactions. A Molecular Mechanics approach was used to evaluate the optimal dihedral angles (Table 2) for each glycosidic junction, and the calculations were performed for a dielectric constant $\varepsilon = 80$, as an approximation for the bulk water. Energy maps were calculated by employment of the DRIV utility (modulated with the DEBG option 150, which instructs the program to start each incremental minimisation reading the initial input structure file). In detail, for each disaccharide entity, both Φ and Ψ were varied incrementally by use of a grid step of 18°, each (Φ, Ψ) point of the map was optimized by use of 2000 P.R. conjugate gradients, Φ is defined as H1−C1−O−$C_{aglycon}$ (or C1−C2−O−$C_{aglycon}$ for Kdo) and Ψ as C1−O−$C_{aglycon}$−$H_{aglycon}$ (or C2−O−$C_{aglycon}$−$H_{aglycon}$ for Kdo). When a Kdo residue was present in a disaccharide, two different maps were calculated (i.e., one for each carboxylic orientation).
The plotting and the analysis of the adiabatic surfaces were performed with the 2D-plot facility incorporated in the MacroModel package, results are reported in Table 2, and all relaxed maps are reported as Supporting Information.
On the base of the values obtained, the complete core oligosaccharide (without the lipid A unit) was constructed by employment of the optimal dihedral angles found (when two minima were present, the lower in energy was considered), and again minimised with MM3* force-field, but with approximation of water solvent by use of the GB/SA model. Molecular Dynamics simulation was started from this optimized structure, initially subjected to an equilibration time of 100 ps, and successively kept in a thermal bath at 303 K for 4000 ps. A dynamic time step of 1.5 fs together with the SHAKE protocol to the hydrogen bonds was applied and coordinates were saved every 4 ps of simulation, resulting in the collection of 1000 structures. Ensemble average distances between the mentioned inter-residue proton pairs were calculated from the Dynamics simulation by use of the two programs NOEPROM[31] (NOE simulations and coordinate extraction) and ORIGIN.
Molecular Dynamic calculations were performed with MM3* force-field and with simulation of the water solvent with the GB/SA model.
Simulations were run for 8 ns at a constant temperature of 300 K, and coordinates were saved every 8 ps, producing a collection of 1000 structures.

Extraction of dihedral angle values was achieved with the SuperMap program provided with the Noeprom software package, whereas visualization and plotting was executed with the Origin program.

## Acknowledgments

We thank Hans-Peter Cordes for recording the NMR spectra, Hermann Moll for help with methylation analysis, and Dr. Sven Müller-Loennies for valuable discussions. We thank Dr. V. Piscopo from the NMR section of the C.I.M.C.F. of the University of Naples "Federico II" for $^{31}P$ NMR spectra and the "Modellistica Computazionale" section of C.I.M.C.F. for computational software facilities. This work was financially supported (M.P.) by MIUR -Roma- (Progetto di Ricerca di Interesse Nazionale 2002). Finally, A.M and C.D.C. thank Prof. Jesus Jimenez-Barbero for useful discussions that contributed considerably to improve the quality of this paper.

[1] C. Alexander, E. T. Rietschel, *J. Endotoxin Res.* **2000**, *7*, 167−202 and references cited therein.
[2] O. Holst, in *Endotoxin in Health and Disease* (Eds.: H. Brade, D. C. Morrison, S. Opal, S. Vogel), Marcel Dekker Inc., New York, **1999**, pp. 115−154.
[3] O. Holst, *Trends Glycosci. Glycotechnol.* **2002**, *14*, 87−103.
[4] F. E. Di Padova, D. Heumann, M. P. Glauser, E. T. Rietschel (Eds.: H. Brade, D. C. Morrison, S. Opal, S. Vogel), Marcel Dekker Inc., New York, **1999**, pp. 633−642.
[5] M. Dow, M. A. Newman, E. von Roepenack, *Annu. Rev. Phytopathol.* **2000**, *38*, 241−261.
[6] J. F. Bradbury, in *Guide to Plant Pathogenic Bacteria*, CAB International Mycological Institute, Kew, England, **1986**.

  

[7] G. Surico, P. Lavermicocca, N. S. Iacobellis, *Phytopathol. Mediterr.* **1988**, *27*, 163−168.
[8] J. J. Barbero, C. De Castro, A. Evidente, A. Molinaro, M. Parrilli, G. Surico, *Eur. J. Org. Chem.* **2002**, *18*, 1770−1775.
[9] A. Molinaro, A. Silipo, R. Lanzetta, M. Parrilli, P. Malvagna, A. Evidente, B. Surico, *Eur. J. Org. Chem.* **2002**, *18*, 3119−3125.
[10] G. I. Birnbaum, R. Roy, J. R. Brisson, H. Jennings, *Carbohydr. Chem.* **1987**, *6*, 17−39.
[11] O. Holst, J. E. Thomas-Oates, H. Brade, *Eur. J. Biochem.* **1994**, *222*, 183−194.
[12] O. Holst, K. Bock, L. Brade, H. Brade, *Eur. J. Biochem.* **1995**, *229*, 194−200.
[13] S. Miertus, J. Bella, R. Toffanin, M. Matulova, S. Paoletti, *J. Mol. Struct. (Theochem)* **1997**, *395−396*, 437−449.
[14] N. J. Palleroni, *Antonie van Leeuwenhoek* **1993**, *64*, 231−251.
[15] Y. A. Knirel, O. V. Bystrova, A. S. Shashkov, B. Lindner, N. A. Kocharova, S. N. Senchenkova, H. Moll, U. Zähringer, K. Datano, G. Pier, *J. Biochem.* **2001**, *268*, 4708−4719 and references cited therein.
[16] G. Seltmann, O. Holst, *The Bacterial Cell Wall*, Springer, Heidelberg, **2001**.
[17] O. Westphal, K. Jann, *Methods Carbohydr. Chem.* **1965**, *5*, 83−91.
[18] R. Kittelberger, F. Hilbink, *J. Biochem. Biophys. Meth.* **1993**, *26*, 81−86.
[19] O. Holst, in *Methods in Molecular Biology, Bacterial Toxins: Methods and Protocols* (Ed.: O. Holst), Humana Press Inc., Totowa, NJ, **2000**, pp. 345−353.
[20] E. V. Vinogradov, O. Holst, J. E. Thomas-Oates, K. W. Broady, H. Brade, *Eur. J. Biochem.* **1992**, *210*, 491−498.
[21] W. Kaca, J. de Jongh-Leuvenink, U. Zähringer, H. Brade, J. Verhoef, V. Sinnwell, *Carbohydr. Res.* **1988**, *179*, 289−299.
[22] O. Holst, W. Broer, J. E. Thomas-Oates, U. Mamat, H. Brade, *Eur. J. Biochem.* **1993**, *214*, 703−710.
[23] M. Süsskind, L. Brade, H. Brade, O. Holst, *J. Biol. Chem.* **1998**, *273*, 7006−7017.
[24] S. Hakomori, *J. Biochem. (Tokyo)* **1964**, *55*, 205−208.
[25] U. Piantini, O. W. Sørensen, R. R. Ernst, *J. Am. Chem. Soc.* **1982**, *104*, 6800−6801.
[26] M. Rance, O. W. Sørensen, G. Bodenhausen, G. Wagner, R. R. Ernst, K. Wüthrich, *Biochem. Biophys. Res. Commun.* **1983**, *117*, 479−485.
[27] D. J. States, R. A. Haberkorn, D. J. Ruben, *Magn. Reson.* **1982**, *48*, 286−292.
[28] A. Bax, M. F. Summers, *J. Am. Chem. Soc.* **1986**, *108*, 2093−2094.
[29] M. F. Summers, L. G. Marzilli, A. Bax, *J. Am. Chem. Soc.* **1986**, *108*, 4285−4294.
[30] N. L. Allinger, Y. H. Yuh, J. H. Lii, *J. Am. Chem. Soc.* **1989**, *111*, 8551−8566.
[31] J. L. Asensio, J. Jiménez-Barbero, *Biopolymers* **1995**, *35*, 55−75.

Received December 20, 2003

  